**International Journal of Computational and Theoretical Chemistry**
2021; 9(2): 32-42
http://www.sciencepublishinggroup.com/j/ijctc
doi: 10.11648/j.ijctc.20210902.12
ISSN: 2376-7286 (Print); ISSN: 2376-7308 (Online)

# Toward Bottom-up Optoelectronic Design of Increasing Fluorination Low Bandgap in *PDTPQ$_X$-types* Copolymers for Organic Photovoltaics Devices

**Simplice Koudjina[1, 4, *], Affi Sopi Thomas[2], René Sawadogo[3], Nobel Kouakou N'Guessan[2], Wilfried Gbèdodé Kanhounnon[1], Gaston Assongba Kpotin[1], Guy Yacolé Sylvain Atohoun[1]**

[1]Laboratory of Theoretical Chemistry and Molecular Spectroscopy (LACTHESMO), University of Abomey-Calavi, Abomey-Calavi, Benin

[2]Laboratory of Thermodynamic and Physico-Chemistry of Medium (LTPCM), University of Nangui Abrogoua, Abidjan, Ivory Coast

[3]Laboratory of Molecular Chemistry and Materials (LCMM), University of Ouagadougou, Ouagadougou, Burkina-Faso

[4]National School of Applied Biosciences and Biotechnologies (ENSBBA), National University of Sciences, Technologies, Engineering and Mathematics (UNSTIM), Abomey, Benin

## Email address:

simplice.koudjina@unstim.bj (S. Koudjina)

[*]Corresponding author

## To cite this article:

Simplice Koudjina, Affi Sopi Thomas, René Sawadogo, Nobel Kouakou N'Guessan, Wilfried Gbèdodé Kanhounnon, Gaston Assongba Kpotin, Guy Yacolé Sylvain Atohoun. Toward Bottom-up Optoelectronic Design of Increasing Fluorination Low Bandgap in *PDTPQ$_X$-types* Copolymers for Organic Photovoltaics Devices. *International Journal of Computational and Theoretical Chemistry*. Vol. 9, No. 2, 2021, pp. 32-42. doi: 10.11648/j.ijctc.20210902.12

**Received**: August 2, 2021; **Accepted**: August 13, 2021; **Published**: September 9, 2021

**Abstract:** Organic photovoltaic performance has been investigated about the fluorination effects as one part on the optoelectronic properties. The quantum chemical accuracy of the optoelectronic and structural properties based on D-A (Donor-Acceptor) conjugated copolymers as PDTPQ$_X$-type (Poly-dithieno-pyrrol-Quinoxaline) has been tediously exposed. The Donor-Acceptor in the copolymers was in our case constitutes to the Donor part in the photovoltaic device, while the Acceptor starting is the PC$_{60}$BM in the same device, which composed the photovoltaic solar cells. The choice of the Donor part in the copolymers was obtained by their HOMO-LUMO bandgap and UV-visible absorption. The bandgap of the Donor part must be higher than that of the Acceptor part for an untroubled charges transfer from the Donor to the Acceptor according to the photovoltaic principle. The substitution of fluorine atoms (0F, 1F, 2F) on the quinoxaline constituents is an effective way to low the HOMO and LUMO energy levels of the alternating copolymers. This fluorine effect has been explored on the optoelectronic properties such as the HOMO-LUMO band gap $E_{gap}$ energy, the fill factor *FF*, the open circuit voltage $V_{oc}$, the electron transfer energy $\Delta E_{et}$, the excitation energy $\Delta E_{ex}$, the absorption wave length $\lambda$ and the oscillator strength *OS*. The equilibrium geometry at the ground state, the electronic structures as the frontier orbital isosurface have been obtained under the caster of the density functional theory (DFT) assist by the time-dependent density functional theory (TD-DFT) with M05 as exchange-correlation functional to come with 6-311G(d,p) basis set. Calculations were performed both in vaccuum and Chlorobenzene (CB) solvent with IEFPCM quantum model. All this has been done with the aim to enhance the energy gap, the $V_{oc}$ values and the fill factor *FF*, which exposed the nanomorphology as the topology of the solar cells photoactive layers. The results of this study show that these promote compounds systems as in the fluorination order are excellent candidates to build photovoltaic device in aim to enhance the open-circuit voltage for donor-acceptor heterojunctions used in organic solar cells.

**Keywords:** Fluorination, *PDTPQ$_x$-types*, Bandgap, UV-VIS Absorption, TD-DFT

## 1. Introduction

A technical challenge for improving bulk heterojunction solar cells performances, based on polymer-fullerene blends as typical semiconductor is to clarify a comprehensive understanding of the fundamental relationship between the morphology surface of the phase-separated blend and the

photophysics of the excited states involved in the charge transfer process [1-4]. However, the morphology surface appreciations and the photophysics behavior of the semiconductor are related to their efficiency for applicability in the polymer light emitting diodes, organic transistors and photovoltaics [5, 6]. Among these, conjugated polymers with high optoelectronic properties are of great important either scientifically and technologically because of their improved light harvesting ability from the solar emission spectrum in photovoltaic devices [7, 8]. In this aspect, the molecular band gaps are parameters of central importance when determining possible applications of conducting polymers [9, 10]. In fact, the molecular band gap control is essential to enhance electroluminescence of organic light-emitting diodes (OLED) [11] as well to improve the efficiency of light absorption in photovoltaic cells [12]. The search for materials with small band gaps has been motivated, by the need to develop organic polymers semiconductors with high electrical conductivity [13, 14]. The quantum chemical calculations with Kohn-Sham (KS) formalism [15] play an important role in studies of polymer materials, which is a great need to establish reliable, instructive and computationally efficient theoretical tools to predict electronic and optical properties of π-conjugated polymers. The main limitation of organic photovoltaic materials is their low efficiency. Nevertheless, their tenable electronic and optical properties, low-cost, high flexibility, versatility of synthetic chemistry [16] entitled them to be prominent candidates in the future market of optoelectronic devices, as substitutes for their inorganic counterparts [17, 18]. To be economically viable and competitive, it is crucial to increase this effectiveness. In order to reach this target, we need to find organic compounds, which have the most relevant electronic properties, including optimum band gap and energy levels allowing effective heterojunction. Scharber et *al*. proposed a semi-empirical model in 2006 to explain the operation of the organic devices and provide an efficiency maximum of 11% based on this model [19]. This Scharber model exposed the theoretical $V_{oc}$ calculation, with the margin error of the charge recombination at 0.3V. Furthermore, the fill factor (*FF*) has been evaluated under Green [20] empirical expressions.

In this investigation, the control of the band-gap and the position of HOMO and LUMO levels of the studied systems are extremely important. For instance, the open circuit voltage $V_{oc}$ and the energy difference between the HOMO level of the donor and LUMO level of the acceptor are related with each other. In fact, the active layers in organic solar cells typically consist of two π-organic materials: a Donor (D) moiety rich in electron and a Acceptor (A) moiety poor in electron, assembled either into a bi-layer structure or in the form of a blend [21]. Fullerene: (6,6)-phenyl-$C_{61}$-butyric acid methyl ester ($PC_{60}BM$ or $PC_{71}BM$) [22, 23] and its derivatives are the most used as electron-acceptor materials [24, 25]. This bi-layer structure is sandwiched between two electrodes. Generally, the Anode is made of Indium Tin Oxide (ITO) and the Cathode of Aluminum (Al**)** [26]. Moreover, bulk heterojunction configuration of the Donor-Acceptor cell is currently the most used device architecture in the organic photovoltaic field due to its good power conversion efficiency (PCE), which is more than 12% [27].

The present work aims to investigate structural electronic properties, absorption spectra and the morphology surface of PDTPQx-type copolymers (Poly-dithieno-pyrrol-Quinoxaline) compounds, non-fluorinate, mono-fluorinate and di-fluorinate [28] on the Quinoxaline lateral chain (Figure 1), by using quantum chemical modeling methods investigated with efficient experimental data.

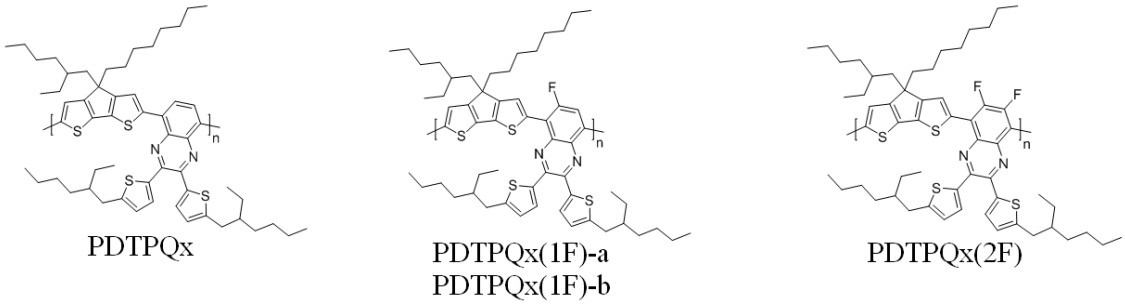


***Figure 1.*** *Molecular structures of polymers PDTPQx(0F), PDTPQx(1F-a, 1F-b as the possible position of F atom on the quinoxaline benzene cycle) and PDTPQx(2F) as modeling in chemical approach.*

## 2. Computaional Details

In the caster of Density Functional Theory (DFT) modeling conceptions and Time Dependent-Density Functional Theory (TD-DFT) [29, 30] implemented in Gaussian09 *ab initio* quantum chemical software package [31] and GaussView.5.0.8 visualization program [32], the ground state geometries of molecular system $PDTPQ_X$-type were optimized in gaseous state and in the solvent, using M05 hybrid functional exchange-correlation functional [33], [34], along with 6-311G(d,p) basis set [35, 36] for all atoms (C, N, O, S, H) into the molecular system explored at the temperature 298.15K and P = 1 atm. Moreover, time-dependent density functional theory (TD-DFT) calculations were performed to allow an estimation of the wavelengths at which electronic transitions take place upon excitation [37]. Single-point TD-DFT calculations for the first 100 singlet–singlet vertical transitions were carried out

using the optimized geometries of the systems to generate the UV-visible spectra. The solvation effects including the Integral Equation Formalism (IEF) [38-41] version of the Polarizable Continuum Model (PCM) [42-44] were used to emulate a dielectric environment for the Chlorobenzene (CB) solvent. After benchmarking, we found that the M05/6-311G(d,p) method provided the best correlation to the experimental data. Our process began with structural optimization of each PDTPQx-type copolymers at the M05 functional level and at TD-DFT level of the UV-visible absorption spectroscopy and the optoelectronic properties. We are using the equilibrium geometric structure to assume that the structural modifications as the torsion of each system would be minimal, which haven't some perturbations on the intrinsic optoelectronic properties [45]. In the calculations, the large alkyl chains were substituted by methyl groups, which reduce the time required for the calculations without impacting the results. Using the optimized geometries, the energies and the topologies of HOMO and LUMO, the band gap $E_g$ and the open-circuit voltage $V_{oc}$ data were determined via the isosurface of the frontier orbital in the gaseous and solvent state.

# 3. Results and Discussion

### *3.1. Molecular Design and Geometric Properties*

The choice of a photovoltaic material is subjective to the principles of voltage and charge transfer of excitons within it, as shown in Figure 2, through the energy levels HOMO and LUMO in the direction of displacement of electrons and holes. It is bester to respect the state of the photovoltaic cell to UV-visible absorption for the purpose of building a photovoltaic device. This method of choice is not exhaustive for any organic photovoltaic solar cell. In our work, we have adopted this method in order to stay within the standards of choosing a photovoltaic solar cell. Other more experienced techniques can be explored, as the goal is to find an organic photovoltaic material for the efficient conversion of solar energy into electricity or light.

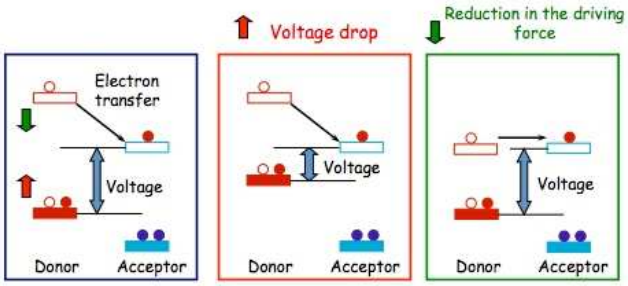


***Figure 2.*** *State of measurement of charge transfer and voltage in the sense of choosing a photovoltaic material.*

The technical aspect of the isolated choice of a solar cells whose electron Donor part is applied to these PDTPQx copolymers. It is here to build the electron Donor as a copolymer that will be used in the photovoltaic device. The two compartments (donor and acceptor) of the copolymer (Figure 3) form the Donor part used in photovoltaic device and the Acceptor part of the same device is including the $PC_{60}BM$ part (Figure 4).

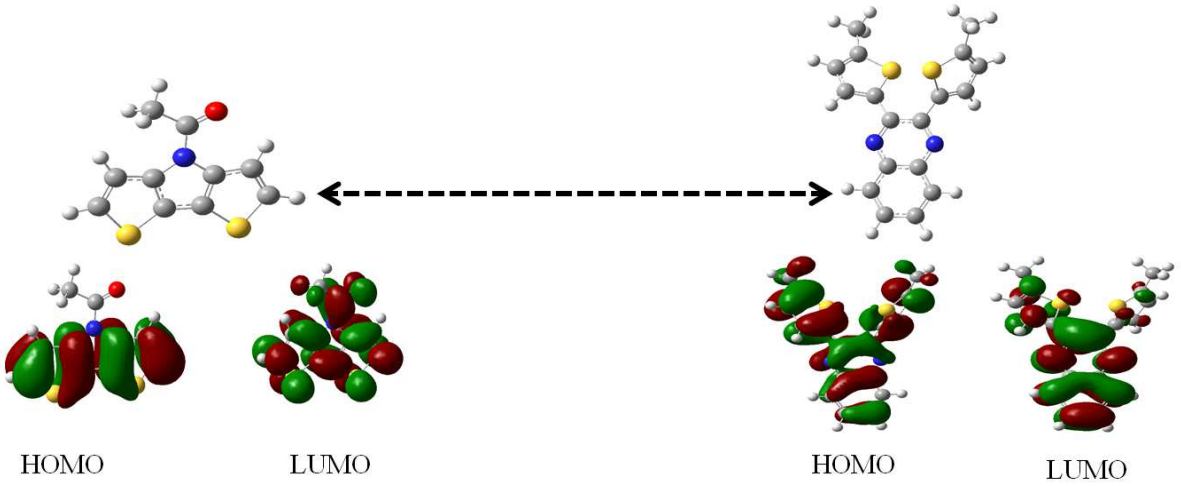


***Figure 3.*** *Donor and Acceptor compartment in the copolymer PDTPQx-type.*

Thus presented in Table 1, the Gap energy of the Donor (4.84 eV) must be greater than that of the Acceptor (4.11 eV) in order to allow an untroubled transfer of charge carriers (electrons and holes), aiming the displacement of the electrons towards the LUMO of the Acceptor and the holes towards the HOMO of the Donor. The Donor thus built in the device, can then undergo an increasing substitutions of fluorine atoms (F) on its quinoxaline part for to enhance the open-circuit voltage $V_{oc}$.

***Table 1.*** *The energies of the HOMO and LUMO levels and the energy Gap in the PDTPQx copolymer.*

| | DTP-Donor | DTP-Acceptor |
|---|---|---|
| $\varepsilon_{HOMO\ (eV)}$ | - 6.01 | - 6.20 |
| $\varepsilon_{LUMO\ (eV)}$ | - 1.17 | - 2.09 |
| $\Delta\varepsilon_{LUMO\text{-}HOMO\ (eV)}$ | 4.84 | 4.11 |

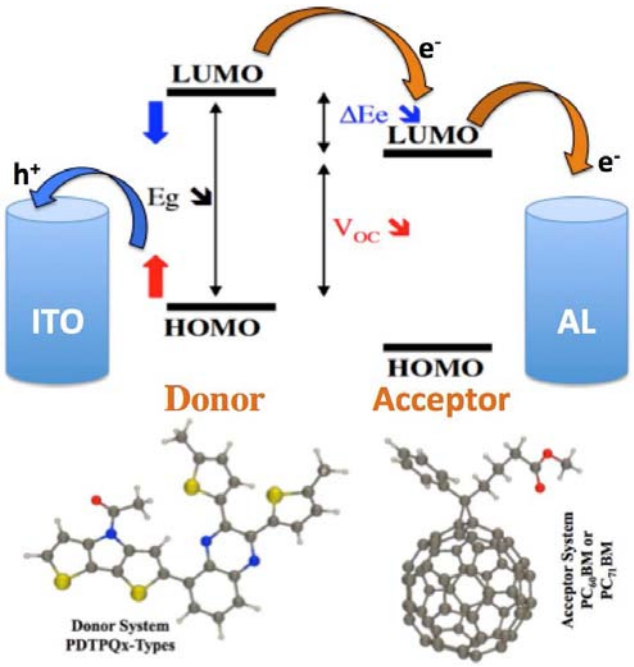


***Figure 4.*** *Chemical Structures of Donor PDTPQ$_x$-types and Acceptor PC$_{60}$BM in below and Displacement of charge carriers and related parameters in a photovoltaic device.*

The ground states geometrical characteristics of the optimized structures of six fluorinates PDTPQx-type copolymers (3 monomers and 3 dimers) depicted in Figure 1 and optimized geometries plotted in Figure 4 by quantum chemical method M05/6-311G(d,p) in the goal to determine their optoelectronic parameters at the relaxation energies. Prior to the monomers optimization, the gaps energy between the HOMO levels of the donor and the acceptor have been calculated to verify the fact that the HOMO and the LUMO levels of the donor must be higher than that of the acceptor for them to form a monomer. This investigation made for parts identified to play the role of donor and acceptor revealed that they could effectively be associated to form monomers with the part of thiophene-combined rings [46]. Secondly, we combined this both parts to have the monomer at the relaxation energy. Thirdly, the succession of several monomers unit constitutes the polymers (Figure 5). The one obtained from the combinations of two monomers were designated by dimer. Monomers differ by the number of substituted fluorine atoms on the acceptor part at the Quinoxaline lateral part. There are two equivalents substitution position on the Quinoxaline part, given that fluorine atom in anyone of both position has no difference on the stability and the structural properties of the molecular system.

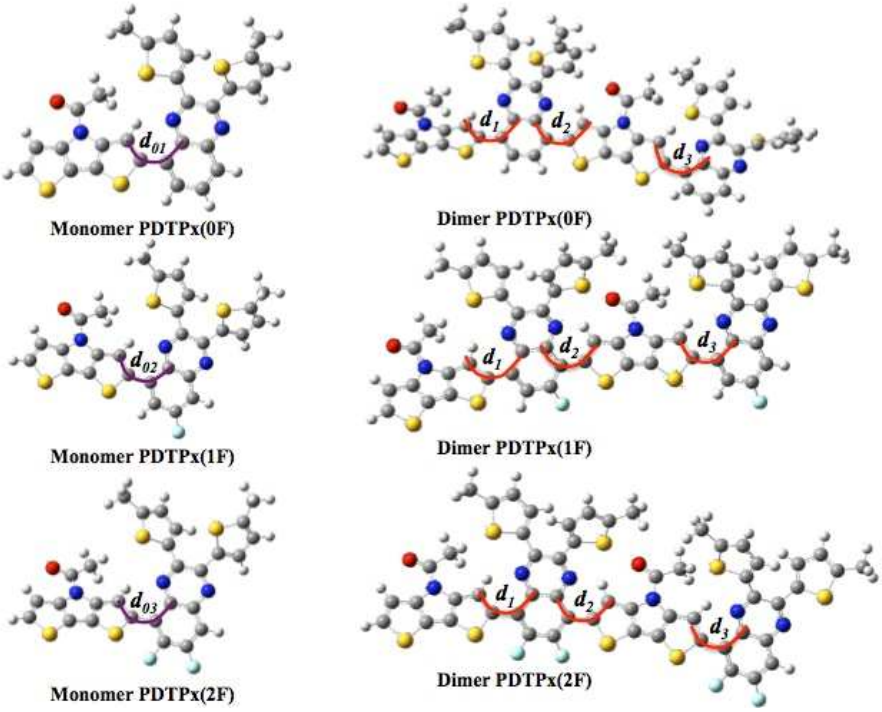


***Figure 5.*** *The most stable PDTPQx-type of the monomers and the dimers at the increase fluorinate substitution on the molecular system. The molecular system, without fluorine atom is as a witness to design the fluorinate effect under the substitution. These optimized system are realized at the gaseous (vacuum) state and at the solvent state of the quantum chemical approach.*

The optimized geometries for studied oligomers show that all oligomers as in the monomers and in the dimers (0F) possess almost planar freeze torsional angles $d_{01} \simeq d_{02} \simeq d_{03}$. This value is relatively low in the dimers part due to the length of the PDTPQx chain with the steric hindrance effect caused by hydrogen atoms in thiophene rings on the quinoxaline part. The planeness has been enhanced with the fluorine atoms substitution on the dimers (1F, 2F) chain as freeze torsion angles $d_1 \simeq d_2 \simeq d_3$ (Table 1).

The geometric parameters show that the planeness of all fluorinate structure (1F and 2F) was almost high of attempts of the donor and acceptor moiety.

***Table 2.*** *Geometric properties: Torsion angle (°) values of the studied monomers and dimers PDTPQx-types compounds optimized with the quantum chemical method M05/6-31G(d,p), at the relaxation energy of the system in order of fluorine atoms substitution on the Quinoxaline lateral moiety.*

| PDTPQx-type | Dimers | | | Monomers | |
|---|---|---|---|---|---|
| | $d_1$ (°) | $d_2$ (°) | $d_3$ (°) | | |
| PDTPQx(0F) | 34.28 | 27.82 | 33.21 | $d_{01}$ (°) | 37.57 |
| PDTPQx(1F) | 146.23 | 145.07 | 144.70 | $d_{02}$ (°) | 29.14 |
| PDTPQx(2F) | 139.56 | 144.59 | 142.21 | $d_{03}$ (°) | 38.38 |

According to Table 2, the values of the torsion angles in the neutral state for the *PDTPQ$_x$-types* with linear chain show that the optimized structure is not totally planar in the monomers with a medium-sized $d_{0X}$ (35.03°) and in the dimers with a medium-sized $d_X$ (31.77° -145.33° -142.12°) in spite of fluorinate effects. The analysis of these results shows that the length of the chain alkyl has low significant effect on the conformation of the structure of the studied *PDTPQ$_x$-types*.

### *3.2. Analysis of Frontier Molecular Orbitals*

The electronic contour of isosurface plots HOMO and LUMO orbitals of the three monomers and three dimers in increasing of the Quinoxaline lateral side fluorination obtained by M05/6-311G(d,p) are shown in Figure 6. We observed on the isosurfaces orbitals that the HOMO orbital is concentrated on the donor part and develop an anti-binding character either on monomers or on dimers. The LUMO orbital, concentrated on the acceptor part, develop in contrast a binding character. These LUMO orbitals are characterized by a delocalized electronic distribution along the compounds skeleton. Such distribution of molecular orbitals suggest that electric conduction would result of the $\pi \rightarrow \pi^*$ transition.

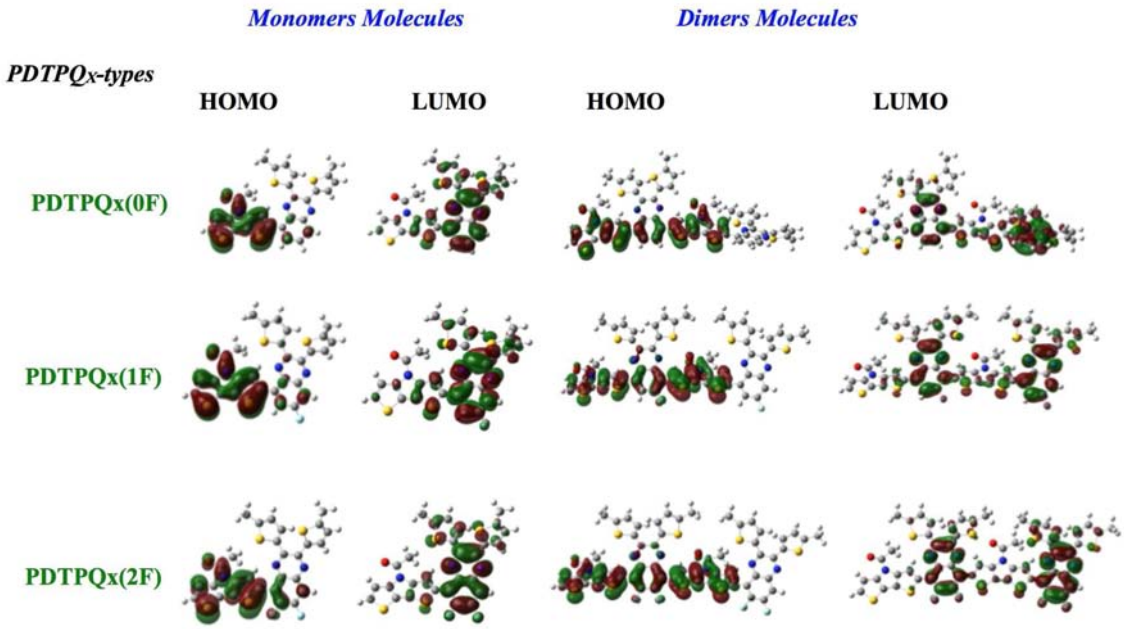


***Figure 6.*** *Occupied-Unoccupied frontier molecular orbital pair contributions to the lowest-energy singlet transition, from level of TD-DFT data for PDTPQx monomers and dimers molecules. Isosurface values are ± 0.02 a.u for the orbital plots.*

### *3.3. Quantum Chemical Parameters of PDTPQ$_x$-types*

The knowledge of the chemical reactivity parameters is very important to understand more details on the chemical structures of the donor and the acceptor part. By using HOMO and LUMO energy values for a molecule, chemical potential (μ), chemical hardness (η) [47], electronegativity (χ) and electronegativity power (ω) can be calculated as follows [48]:

$$\eta = \frac{(E_{LUMO} - E_{HOMO})}{2}; \mu = \frac{(E_{HOMO} + E_{LUMO})}{2}; \chi = -\frac{(E_{HOMO} + E_{LUMO})}{2}; \omega = \frac{\mu^2}{2\eta}$$

On the acceptor part, we note that the $PC_{60}BM$ has the smallest value of the chemical potential ($\mu = -5.10\ eV$) compared to three P*DTPQ$_x$-types* compounds (Table 3). This is a tendency to view the electrons to escape from those compounds has a high chemical potential to $PC_{60}BM$ which has a small chemical potential. Therefore, $PC_{60}BM$ behaves as an acceptor of electrons and other compounds behave as a donor of electrons. As for the electronegativity, we notice that the $PC_{60}BM$ has a higher value of electronegativity (5.10 eV) than other compounds. This indicates that the $PC_{60}BM$ is able to attract the electrons from other studied compounds. The compound $PC_{60}BM$ has $\eta$ greater than other

compounds. This indicates that $PC_{60}BM$ finds it difficult to liberate the electrons, while the other compounds are the best candidates to liberate an electron to the $PC_{60}BM$. Finally, we notice that the compound $PC_{60}BM$ is more electrophilic compound than other compounds, which shows the lowest values of $\omega$. Therefore, these compounds are better electrons donors in photovoltaics device.

***Table 3.*** *Electronic properties parameters, chemical hardness (η), chemical potential (μ), electronegativity (χ) and electronegativity power (ω) obtained by M05/6-311G(d,p) of the studied molecules.*

| **Monomers / Dimers Compounds** | | | | |
|---|---|---|---|---|
| ***PDTPQ$_x$-types*** | $\eta(eV)$ | $\mu(eV)$ | $\chi(eV)$ | $\omega(eV)$ |
| PDTPQx-(0F) | 1.76 / 1.50 | -4.02 / -3.96 | 4.02 / 3.96 | 4.59 / 5.23 |
| PDTPQx-(1F) | 1.75 / 1.60 | -4.10 / -4.02 | 4.10 / 4.02 | 4.80 / 5.05 |
| PDTPQx-(2F) | 1.76 / 1.60 | -4.13 / -4.08 | 4.13 / 4.08 | 4.85 / 5.20 |
| $PC_{60}BM$ | 1.80 | -5.10 | 5.10 | 7.23 |

### *3.4. Optoelectronic and Photovoltaics Properties Analysis*

The absorption of a new material matches with the solar spectrum is an important factor for the application as a photovoltaic material. Also, a good photovoltaic material should have broad and strong visible absorption characteristics. However, the optoelectronic properties depend essentially on the appropriate HOMO and LUMO energy levels and the electron and hole mobilities. On the other hand, the energy band gap ($E_{gap}$) between the Highest Occupied Molecular Orbital (HOMO) and the Lowest Unoccupied Molecular Orbital (LUMO) is an essential parameter that determines the molecular admittance since it is a measure of the electron density hardness. This band gap of the organic photovoltaic compounds is estimated as the difference between the HOMO and the LUMO level energies on the ground singlet state.

In addition, the bulk-heterojunction (BHJ) cells combine the advantages of easier fabrication and higher conversion efficiency due to the considerably extended D/A interface. The BHJ solar cells have been essentially based on the use of soluble π-conjugated (done) polymers as donor material, owing to a useful combination of optical and charge-transport properties. However, besides the limit imposed to the maximum conversion efficiency by its intrinsic electronic properties, PDTPQx-type and more generally polymers pose several problems related to the control of their structure, molecular weight, polydispersity, and purification [49].

The results of the experiment showed that the HOMO and LUMO energies were obtained from an empirical formula based on the onset of the oxidation and reduction peaks measured by cyclic voltammetry [50, 51]. However, theoretically the HOMO and LUMO energies can be calculated by DFT level of calculation. It is remarkable that the solid–state packing effects are not calculated in DFT calculations, this fact affects the HOMO and LUMO energy levels in a thin film compared to an isolated molecule as considered in the calculations. Though these calculated energy levels lack some accuracy still we can use them to get information by comparing similar copolymers [52] as candidate for photovoltaic device. In Table 4, we listed the calculated parameters for the PDTPQx-type at ground state.

In order to determine optoelctronic properties of these PDTPQx-type copolymers, we have investigated the transition energy as HOMO-LUMO band gap:

$E_{gap} = E_{HOMO} - E_{LUMO}$, which highlight the light emission. The open circuit voltage $V_{OC}$ which evaluates the possibilities of electron transfer from the HOMO of the electron donor to the LUMO of the electron acceptor, that taking into account the energy lost during the photo-charge generation [53, 54]. The theoretical values of open-circuit voltage $V_{OC}$ have been calculated from the following expression [19]:

$V_{oc} = \frac{1}{e}\left(|E^{D}_{Donor}| - \left|E^{PCBM}_{Acceptor}\right| - 0.3\right)$. The fill factor FF, which one of the key parameters in determining the efficiency of solar cell photovoltaic [55]. Therefore, the expression for Fill Factor [20] can be determined empirically as:

$FF = \frac{V_{oc} - ln(V_{oc}+0.72))}{V_{oc}+1}$. On the other hand and knowing that in organic solar cells, the open-circuit voltage is found to be linearly dependent on the HOMO level of the donor and the LUMO level of the acceptor [56]. The power conversion efficiency PCE was calculated according to the following equation: $PCE = \frac{1}{P_{in}(FF.V_{oc}.J_{sc})}$.

Where $P_{in}$ is the incident power density, $J_{sc}$ is the short-circuit current, $V_{oc}$ is the open-circuit voltage and $FF$ denotes the fill factor. The electron transfer energy $\Delta E_{et}$ from the LUMO level of the donor to LUMO level of the acceptor is expressed as:

$\Delta E_{et}(eV) = E^{LUMO}_{Donor} - E^{LUMO}_{Acceptor}$. The excitation energy $\Delta E_{ex}$, as the absorption response of the UV-visible absorption was calculated according to the following equation:

$\Delta E_{exc} = \frac{hC}{\lambda(nm)} = \frac{1240}{\lambda(nm)}$. The quantum efficiency (QE) refers to the percentage of photons that are converted to electric current when the cell is operated under short circuit conditions. Two different QE are usually measured, the external (EQE) and internal (IQE) quantum efficiency. Since all the photons captured by the cell do not contribute to electric current, the EQE is introduced to quantify the fraction of incident photons that are converted to electric current at a given wavelength. The internal quantum efficiency IQE is defined as the fraction of absorbed photons that are converted to electric current at a given wavelength. Note that recombination losses make up a portion of the internal quantum efficiency. The external quantum efficiency EQE can be easily expressed as:

$EQE(\lambda) = \frac{J_{sc}(\lambda)}{\phi(\lambda)} \times \frac{hC}{e\lambda}$, where $J_{sc}(\lambda)$ is the short-circuit current density for the wavelength $\lambda$.

***Table 4.*** *Experimental electrochemical properties determined by cyclic voltammetry (CV) and UV-vis data of the PDTPQ$_x$-types in chlorobenzene (CB) solvent under the fluorination effects and a comparison between their DFT-calculated frontiers orbital energies. Excitation energies $\Delta E_{exc}$ (eV), Wavelengths λ (nm), Oscillator strength (OS) and Electronic Transitions of the absorption maxima of each PDTPQx compounds.*

| Monomers PDTPQx-type | | | | | | | | | |
|---|---|---|---|---|---|---|---|---|---|
| PDTPQx | $E_{HOMO}$/Exp(eV) | $E_{LUMO}$/Exp(eV) | $E_{gap}$/Exp(eV) | $\Delta E_{et}$(eV) | $V_{oc}$(V) | $\Delta E_{exc}$(eV) | FF | $\lambda_{max}$(nm) | *OS* |
| PDTPQx(0F) | - 5.77/-5.18 | - 2.26/-3.34 | 3.51/1.84 | 1.94 | 1.27 | 2.70 | 0.256 | 459.51 | 0.337 |
| PDTPQx(1F) | -5.84/-5.31 | -2.35/-3.40 | 3.49/1.91 | 1.85 | 1.34 | 2.68 | 0.264 | 462.26 | 0.399 |
| PDTPQx(2F) | - 5.86/-5.50 | - 2.43/-3.45 | 3.43/2.05 | 1.77 | 1.36 | 2.65 | 0.268 | 467.09 | 0.369 |
| Dimers PDTPQx-type | | | | | | | | | |
| PDTPQx | $E_{HOMO}$(eV) | $E_{LUMO}$(eV) | $E_{gap}$ (eV) | $\Delta E_{et}$(eV) | $V_{oc}$(V) | $\Delta E_{exc}$(eV) | FF | $\lambda_{max}$/Exp (nm) | *OS* |
| PDTPQx(0F) | -5.44 | -2.45 | 2.99 | 1.75 | 0.89 | 2.29 | 0.219 | 542.30/684 | 1.330 |
| PDTPQx(1F) | -5.52 | -2.50 | 3.02 | 1.70 | 1.22 | 2.38 | 0.251 | 520.18/661 | 1.154 |
| PDTPQx(2F) | -5.63 | -2.53 | 3.10 | 1.67 | 1.30 | 2.39 | 0.260 | 519.26/646 | 1.161 |
| $PC_{60}BM$ | -6.0 | -4.2 | 1.8 | | | | | | |
| | *Electronic Transition* | | | | | *Contribution* | | | |
| | HOMO ----------> LUMO | | | | | 68% | | | |
| *PDTPQx(0F)* | HOMO ----------> LUMO + 2 | | | | | 56% | | | |
| | HOMO – 1 ----------> LUMO + 4 | | | | | 51% | | | |
| | HOMO ----------> LUMO | | | | | 68% | | | |
| *PDTPQx(1F)* | HOMO ----------> LUMO + 4 | | | | | 32% | | | |
| | HOMO – 2 ----------> LUMO | | | | | 47% | | | |
| | HOMO ----------> LUMO | | | | | 68% | | | |
| *PDTPQx(2F)* | HOMO ----------> LUMO + 4 | | | | | 52% | | | |
| | HOMO – 2 ----------> LUMO | | | | | 49% | | | |

The theoretical electronic properties parameters are listed in Table 4. The $E_{gap}$ is much affected by the substitution of fluorine in the donor unit. These results can be explained by the electron-withdrawing power of the acceptor units $PC_{60}BM$ introduced in each copolymers chain. This implies that different side substituent structures play key role in electronic properties and the effect of slight structural variations. It can also be found that, the HOMO and LUMO energies of the studied compounds are slightly different. This implies that different structures play key roles on electronic properties and the effect of slight structural variations, especially the effect of the motifs branched to the molecule on the HOMO and LUMO energies is clearly seen. In addition, energy ($E_{gap}$) of the PDTPQx-type is lower slightly with the fluorination (0F, 1F, 2F) from 3.51 eV to 3.43 eV in the monomers and from 3.00 eV to 3.12 eV in the dimers. Somewhere else, the open-circuit voltage increases slightly in the monomers-type and the dimers-type with the fluorination (0F, 1F, 2F) from 1.27 V to 1.37V in the monomers and from 0.95 V to 1.13 V in the dimers. The electron transfer energy is also lower slightly with the fluorination (0F, 1F, 2F) from 1.94 eV to 1.77 eV in the monomers and from 1.74 eV to 1.68 eV in the dimers. The UV-visible absorption spectroscopy $\lambda_{max}$ increases slightly with the fluorination (0F, 1F, 2F) from 542.30 nm to 519.26 nm in the dimers-type in the same tendency of experimental values from 684 nm to 646 nm. This explained clearly that the aggregate PDTPQx-type materials have the same tendency of voltage variation with the better UV-visible absorption and exposed these solar cell materials to be the potential candidate for organic photovoltaics device.

The analysis of Figure 7 shows that the dimer PDTPQx(2F), which has the lowest energy gap (ΔE = 3.110 eV) in the fluorination series is the most reactive and less stable molecule. Thus, the following sequence polymers of PDTPQx(1F) will be the less reactive and most stable molecule. However, the fluorine atoms substitution in lateral Quinoxaline chain is a real mean to enhance the open-circuit voltage and to heighten the performance of photovolataic devices.

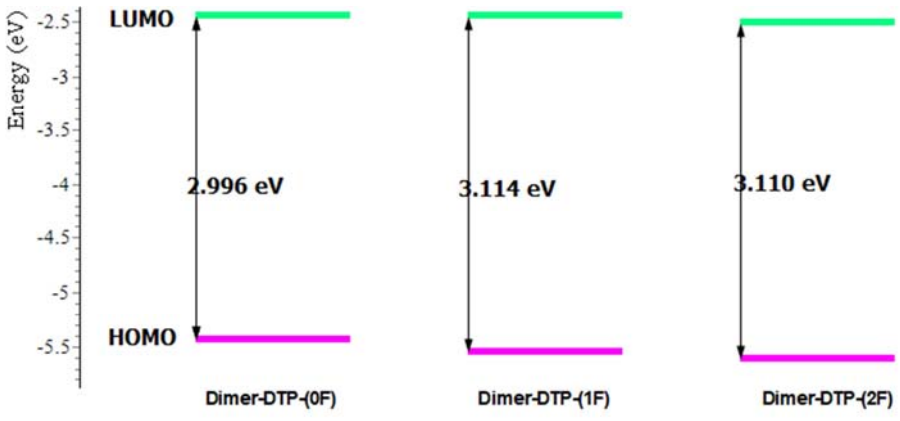


***Figure 7.*** *Energy distribution of HOMO and LUMO levels of PDTPQx-type dimers, observed by Chemissian chemical software package* [57, 58].

The results of quantum calculations indicates that upon addition of fluorine atoms onto the Quinoxaline moiety, both the HOMO and LUMO levels are stabilized, but due to a stronger impact on the former HOMO-LUMO gap slightly opens up with increasing number of fluorine atoms (0F, 1F, 2F). The observed theoretical trends correlate nicely to the experimental results. However, the knowledge of the frontier molecular orbitals is very important to understand more details on excited-state properties. The HOMO and LUMO can then provide a reasonable qualitative indication of the excitation properties and the ability of electron or hole transport [37].

The absorption properties of a new material matches with the solar spectrum is an important factor for the application as a photovoltaic material, and a good photovoltaic material should have broad and strong visible absorption characteristics. The TD-DFT method has been used on the basis of the optimized geometry to obtain the energy of the singlet-singlet electronic transitions and absorption properties $\lambda_{max}$ (nm) of PDTPQx-type. The corresponding simulated UV-Vis absorption spectra of the studied molecules, presented as oscillator strength against wavelength, and the experiment one is shown in Figure 8. As illustrated in Table 4, we can find the values of calculated absorption $\lambda_{max}$ (nm) and oscillator strength (O.S) along with main excitation configuration of all studied molecules.

UV–vis measurements revealed that all polymers show a broad absorption in the visible range of the solar spectrum (Figure 8). For *PDTPQ$_X$-types*, the lowest optical bandgap was observed, with a wavelength of maximum absorption ($\lambda_{max}$) at 684 nm in solution, shifting to 703 nm in thin film. Upon monofluorination PDTPQx (1F), a clear blue-shift was observed [59]. A similar trend, however less pronounced, was seen for the difluorinated copolymer PDTPQx (2F). The electrochemical properties of the three copolymers were investigated by cyclic voltammetry (CV) and their HOMO and LUMO energy levels were determined by the onset of the first oxidation and reduction peaks, respectively (Table 4). Through the introduction of one or two fluorine atoms, the electron withdrawing power of the Qx acceptor increases, leading to a further deepening of the HOMO level. The LUMO levels are affected to a lesser extent, leading to an increased band gap, as also seen in the UV–vis spectra (Figure 8).

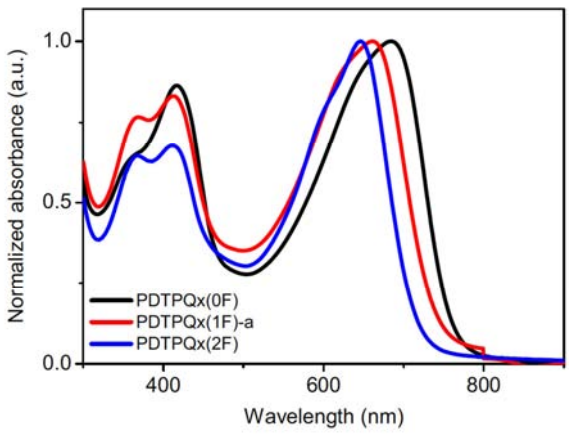


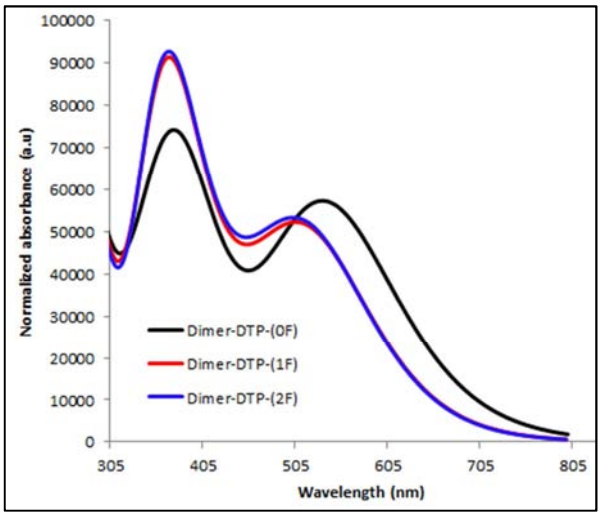


***Figure 8.*** *UV-Vis absorption spectra for all copolymers in CB (Chlorobenzene) solution, at left for the experimental UV-vis spectra and at right calculated spectra of the PDTPQx copolymers, with the fluorination variation.*

To investigate the photovoltaic features of the novel *PDTPQ$_x$-types* copolymers, blends were prepared in combination with $PC_{71}BM$ and these were applied as photoactive layers in BHJ polymer solar cells with a standard configuration (glass/ITO/PEDOT:PSS/active layer/Ca/Al). As represented in Figure 9 and Table 5, the optimized devices (after careful screening of solvent, blend ratio and active layer thickness) based on PDTPQx:$PC_{71}BM$ (1:3 ratio in chlorobenzene (CB)) yielded a $V_{oc}$ of 0.67 V, and combined with a $J_{sc}$ of 12.57 mA/cm$^2$ and a FF of 0.54, an average power conversion efficiency (PCE) of 4.53% (best device 4.81%) could be obtained (Table 5, Figure 9). Despite the still modest $V_{oc}$, record device efficiency was obtained for PDTPQx polymer donor materials [60]. A noticeable increase in $V_{oc}$ (to 0.76 V) was observed when combining the monofluorinated PDTPQx(1F) copolymer with $PC_{71}BM$ (Table 4, Figure 7). However, a simultaneous drop in $J_{sc}$ to an average of 6.63 mA/cm$^2$ was observed as well, even after tedious optimization. Eventually, the best performing device for the PDTPQx(1F):$PC_{71}BM$ combination showed a power conversion efficiency of 2.30%. This decrease in $J_{sc}$ cannot be attributed to reduced charge carrier mobility, as photo-induced charge extraction by linearly increasing voltage (photo-CELIV) measurements indicated that the mobilities (in the appropriate direction of the solar cell mode) are in the same (suitable) range for the three copolymer PDTPQx:$PC_{71}BM$ blends and even increase upon Qx fluorination (Table 5).

To investigate if the reduced $J_{sc}$ could be linked to the active layer nanomorphology, AFM imaging was applied, which revealed the formation of large aggregates in the films, even for the best devices (Figure 9). Similar previous observations for fluorinated copolymers have been attributed to the fluorophobicity of $PC_{71}BM$ [61]. Therefore, the aggregates can most likely be ascribed as

$PC_{71}BM$-rich clusters, which is confirmed by the surface ratio (68-75%) matching closely to the polymer:$PC_{71}BM$ 1:3 feed ratio. Aggregation at this large scale (~200 nm) strongly diminishes the donor-acceptor interface available for charge separation. In an attempt to overcome this, a number of processing additives were applied. However, no noticeable improvement in blend nanomorphology (and hence efficiency) could be obtained. It has recently been stated that fluorination of low bandgap copolymers will only lead to enhancements in photovoltaic performance when the *PDTPQ$_x$-types* copolymer molar mass is reasonably high [62].

***Table 5.*** *Photovoltaic performances of (optimized) PDTPQx:$PC_{71}BM$ (1:3) BHJ polymer solar cells and charge carrier mobilities obtained for these devices structures PDTPQ$_x$-types glass/ITO/PEDOT:PSS/active layer/Ca/Al. PEDOT:PSS [poly(3,4-ethylenedioxythiophene):poly(styrenesulfonic acid). The active layer thicknesses for the optimized devices were ~80 – 95 nm. Samples were prepared by dip coating the platinum working electrode in the respective polymer solutions (also used for the solid- state UV–vis measurements).*

| **PDTPQ$_X$:$PC_{60}BM$** | | | | |
|---|---|---|---|---|
| | ***Mobility*** $(cm^2/V.s)$ | $J_{sc}$ $(mA.cm^{-2})$ | $V_{oc}(V)$ | ***PCE***(%) |
| PDTPQx-(0F) | $4.10^{-5}$ | 12.57 | 0.67 | 4.53 |
| PDTPQx-(1F) | $1.10^{-4}$ | 6.63 | 0.76 | 2.30 |
| PDTPQx-(2F) | $1.10^{-3}$ | 3.90 | 0.79 | 1.55 |

Moreover, no further enhancement in $V_{oc}$, as expected from the deepened HOMO level (Table 5), was seen. As illustrated by the AFM images (Figure 10), even larger aggregates were formed during film formation for the PDTPQx(2F):$PC_{71}BM$ blend, which suggests that the overall lower photovoltaic performance can be attributed to the far-from-optimal BHJ blend nanomorphology. However, the nanomorphology still remained unfavourable as compared to the active layer based on the non-fluorinated copolymer. Although there are no large aggregates any more, a quite rough morphology with spike-shaped structures at the surface is formed. Moreover, the enhancement in $V_{oc}$ due to Qx fluorination was completely lost in this case. Nonetheless, combined with a lowering of the $J_{sc}$, poor device properties were still obtained. Furthermore, for both the PDTPQx(1F):$PC_{71}BM$ and PDTPQx(2F):$PC_{71}BM$ active layer blends, the *FF* of the optimized devices was never as high as for PDTPQx:$PC_{71}BM$.

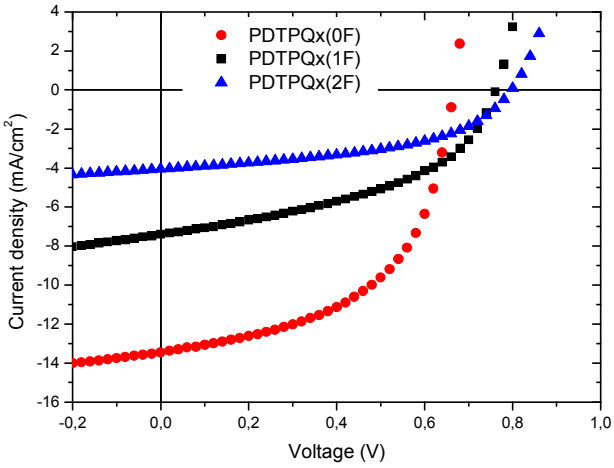


***Figure 9.*** *J-V curves under illumination for the best solar cell devices based on the PDTPQ$_x$-types copolymers.*

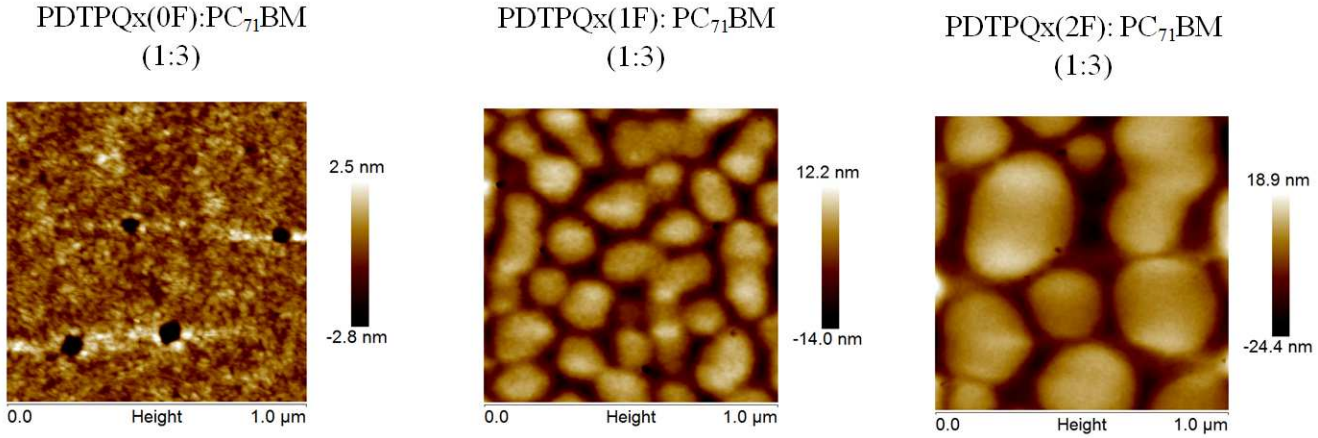


***Figure 10.*** *AFM topography images of the photoactive layers of the PDTPQx:$PC_{71}BM$ solar cells prepared without processing additives. For PDTPQx(0F) the maximum layer bias is 2.5 nm, PDTPQx(1F) the maximum layer bias is 12.2 nm, PDTPQx(2F) the maximum layer bias is 18.9 nm; that was explained the fluorination effect on the nanomorphology observed in the aggregate materials, which enhanced the photovoltaics performance in device.*

## 4. Conclusion

At the end of this work, we have investigated π-conjugated polymers, which are quite versatile in their application to organic electronic devices. Application of quantum chemical calculations has been shown to provide structural and spectroscopic insight into experimentally determined results. By modelling six kind of fluorinate organic material (3 monomers and 3 dimers), with the quantum chemical method M05/6-311G(d,p), comparable optoelectronic predictions have been made and translated into the experimental one to promote the performance of the photovoltaic devices. This modeling method produces simulated the accuracy optoelectronic properties by

increasing the number of fluorine atoms in the lateral quinoxaline Qx chain in the molecular system compared to the experimental spectra. The morphology surface as showing with AFM Microscopy heightened the photoactive layers of the three kind of PDTPQx(0F), PDTPQx(1F) and PDTPQx(2F), that the maximum layer bias is 18.9 nm, obtained in PDTPQx(2F), which was explained the fluorination effect on the nanomorphology observed in the aggregate materials, with enhancement photovoltaic device performance.

## Author Contributions

The manuscript was written through contributions of all authors. All authors have given approval to the final version of the manuscript. These authors contributed equally.

## Conflict of Interest

The authors declare no conflict of interest.

## Acknowledgements

The calculations have been performed on the LACTHESMO (Laboratoire de Chimie Théorique et de spectroscopie Moléculaire) equipment at the University of Abomey-Calavi (UAC) in Benin, with the collaboration of the Laboratory for Chemistry of Novel Materials (CMN) at the University of Mons (UMons) in Belgium. We thank especially Professor. David Beljonne who is our main partner in this fruitful collaboration who made the CECI (Consortium des Equipements de Calculs Intensifs) server available to us.

## References

[1] Liang, Y.; Xu, Z.; Xia, J.; Tsai, S. T.; Wu, Y.; Li, G.; Ray, C.; Yu, L., *Adv. Mater*. 2010, 22, E135–E138.

[2] Scharber, M. C.; Koppe, M.; Gao, J.; Cordella, F.; Loi, M. A.; Denk, P.; Morana, M.; Egelhaaf, H. J.; Forberich, K.; Dennler, G.; Gaudiana, R.; Waller, D.; Zhu, Z.; Shi, X.; Brabec, C. J., *Adv. Mater*. 2010, 22, 367–370.

[3] Benson-Smith, J. J.; Goris, L.; Vandewal, K.; Haenen, K.; Manca, J. V.; Vanderzande, D.; Bradley, D. D. C.; Nelson, J., *Adv. Funct. Mater*. 2007, 17, 451–457.

[4] Shuttle, C. G.; Hamilton, R.; O'Regan, B. C.; Nelson, J.; Durrant, J. R. *Proc. Natl. Acad. Sci*. U.S.A. 2010, 107, 16448–16452.

[5] M. R. Lee; RD Eckert; K Forberich; G Dennler; C. J. Brabec; R. A. Gaudiana, *Science*, 2009, 324, 232-235.

[6] F. Etzold; I. A. Howard; R. Mauer; M. Meister; T. D. Kim; K. S. Lee; N. S. Baek; F. Laquai, *J. Am. Chem. Soc.,* 2011, 133, 9469-9479.

[7] C. J. Brabec, N. S. Sariciftci, J. C. Hummelen, *Adv. Funct. Mater*. 11, 2001, 15-26.

[8] E. Bundgaard, F. C. Krebs, *Sol. Energy Mater. Sol. Cells* 91, 2007, 954-985.

[9] G. Inzelt, Conducting Polymers: *A New Era in Electrochemistry*; F. Scholz, Ed.; Monographs in Electrochemistry; Springer: Berlin Heidelberg, 2008; Chapter 1, pp 1−6.

[10] J. Roncali, *Chem. Rev.* 1997, 97, 173−206.

[11] N. C. Greenham; S. C. Moratti; D. D. C. Bradley; R. H. Friend; A. B. Holmes, *Nature* 1993, 365, 628−630.

[12] J. Gierschner; J. Cornil; H.-J. Egelhaaf, *Adv. Mater*. 2007, 19, 173−191.

[13] B. A. Jones; A. Facchetti; M. R. Wasielewski; T. J. Marks, *J. Am. Chem. Soc*. 2007, 129, 15259−15278.

[14] A. Kohler; D. A. dos Santos; D. Beljonne; Z. Shuai; J.-L. Bredas; A. B. Holmes; A. Kraus; K. Mullen; R. H. Friend, *Nature* 1998, 392, 903−906.

[15] K. Capelle, *Braz. J. Phys*., 2006, 36, 1318-1343.

[16] S. Logothetidis, *J. Mater. Sci. Eng. B*, 2008, 152, 96–104.

[17] L. Tsakalakos, J. Balch, J. Fronheiser, B. A. Korevaar, O. Sulima and J. Rand, *Appl. Phys. Lett.*, 2007, 91 (23), 233117.

[18] J. Müller, B. Rech, J. Springer and M. Vanecek, *Sol. Energy*, 2004, 77, 917–930.

[19] M. C. Scharber; D. Mühlbacher; M. Koppe; P. Denk; C. Waldauf; A. J. Heeger; C. J. Brabec, *Adv. Mater*., 2006, 18, 789-794.

[20] Green M. A., *Solid-State Electronics*. 1981; 24:788-789.

[21] Y. Yi, V. Coropceanu, J. L. Brédas, *J. Am. Chem. Soc*., 2009, 131 (43), 15777-15783.

[22] Lee, J.; Ma, W. L.; Brabec, C. J.; Yuen, J.; Moon, J. S.; Kim, J. Y.; Lee, K.; Bazan, G. C.; Heeger, A. J., *J. Am. Chem. Soc*. 2008, 130, 3619–3623.

[23] Kim, Y.; Choulis, S. A.; Nelson, J.; Bradley, D. D. C.; Cook, S.; Durrant, J. R. *Appl. Phys. Lett*. 2005, 86, 063502–063504.

[24] N. S. Sariciftci, L. Smilowitz, A. J. Heeger, F. Wudl, *Science,* 1992, 258 (5087), 1474–1476.

[25] Y. Li, T. Pullerits, M. Zhao, and M. Sun. *J. Phys. Chem. C,* 2011*,* 115, 44, 21865-21873.

[26] C. W. Tang, *Appl. Phys. Lett*., 1986, 48 (2), 183-185.

[27] http://www.heliatek.com/wpcontent/uploads/2013/01/130116PRHeliatekachieves_OPV.pdf, 2013.

[28] P. Verstappen, J. Kesters, W. Vanormelingen, G. H. L. Heintges, J. Drijkoningen, T. Vangerven, L. Marin, S. Koudjina, B. Champagne, J. Manca, L. Lutsen, D. Vanderzande, W. Maes, *J. Mater. Chem. A*. 2015, 3, 2960–2970.

[29] M. E. Casida, *Low-Lying Potential Energy Surfaces*, 2002, 828, 199–220.

[30] M. A. L. Marques, C. Ullrich, F. Nogueira, A. Rubio, and E. K. U. Gross, volume 706 of Lecture Notes in *Physics, Springer, Berlin*, 2006.

[31] M. J. Frisch, G. W. Trucks, H. B. Schlegel, G. E. Scuseria, M. A. Robb, J. R. Cheeseman, G. Scalmani, V. Barone, B. Mennucci, G. A. Petersson, H. Nakatsuji, M. Caricato, X. Li, H. P. Hratchian, A. F. Izmaylov, J. Bloino, G. Zheng, J. L. Sonnenberg, M. Hada, M. Ehara, K. Toyota, R. Fukuda, J. Hasegawa, M. Ishida, T. Nakajima, Y. Honda, O. Kitao, H. Nakai, T. Vreven, J. A. Montgomery, Jr., J. E. Peralta, F. Ogliaro, M. Bearpark, J. J. Heyd, E. Brothers, K. N. Kudin, V. N. Staroverov, T. Keith, R. Kobayashi, J. Normand, K. Raghavachari, A. Rendell, J. C. Burant, S. S. Iyengar, J. Tomasi, M. Cossi, N. Rega, J. M. Millam, M. Klene, J. E. Knox, J. B. Cross, V. Bakken, C. Adamo, J. Jaramillo, R. Gomperts, R. E. Stratmann, O. Yazyev, A. J. Austin, R. Cammi, C. Pomelli, J. W. Ochterski, R. L. Martin, K. Morokuma, V. G. Zakrzewski, G. A. Voth, P. Salvador, J. J. Dannenberg, S. Dapprich, A. D. Daniels, O. Farkas, J. B. Foresman, J. V. Ortiz, J. Cioslowski, and D. J. Fox, Gaussian, Inc., Gaussian 09, Revision D.01, Inc., Wallingford CT, 2013.

[32] E. Frisch, H. P. Hratchian, R. D. Dennington II, et *al*., 2009 Gaussview, Version 5.0.8, Gaussian, Inc., 235 Wallingford CT.

[33] J. Tomasi, B. Mennucci, R. Cammi, *Chem. Rev*. 105, 2005, 2999–3093.

[34] Y. Zhao, N. E. Schultz and D. G. Truhlar, *J. Chem. Phys*., 2005, 123 (16), 161103.

[35] V. A. Rassolov, J. A. Pople, M. A. Ratner, T. L. Windus, *J. Chem. Phys*, 1998, 109 (4), 1223–1229.

[36] W. J. Hehre, R. Ditchfield, J. A. Pople, *J Chem Phys*, 1972, 56 (5), 2257–2261.

[37] McCormick, T. M.; Bridges, C. R.; Carrera, E. I.; DiCarmine, P. M.; Gibson, G. L.; Hollinger, J.; Kozycz, L. M.; Seferos, D. S. *Macromolecules,* 2013, 46, 3879–3886.

[38] E. Cancès, B. Mennucci, J. Tomasi, *J. Chem. Phys*. 1997, 107 (8), 3032–3041.

[39] B. Mennucci, E. Cancès, J. Tomasi, *J. Phys. Chem. B* 1997, 101, 49, 10506–10517.

[40] S. Miertus, E. Scrocco, J. Tomasi, *Chem. Phys*. 1981, 55 (1), 117–129.

[41] R. Cammi, J. Tomasi, *J. Comput. Chem*. 1995, 16 (12), 1449–1458.

[42] T. Yanai, D. P. Tew, N. C. Handy, *Chem. Phys. Lett*. 2004, 393 (1-3), 51–57.

[43] Klamt, A., Moya, C. Palomar, J., *J. Chem. Theory Comput*, 2015, 11 (9), 4220–4225.

[44] M. Bourass, N. Komiha, O. K. Kabbaj, N. Wazzan, M. Chemek, M. Bouachrine, *New J. Chem*. 2019, 43, 15899–15909.

[45] N. Hergué, C. Mallet, G. Savitha, M. Allain, P. Frère, J. Roncali. *Org. Lett*., 2011, 13, 7, 1762–1765.

[46] Soumia Boussaidi, Hsaine Zgou, Abderrahim Eddiouane, Hassan Chaib, Mohamed, *J. Comput. Methods Mol. Des*., 2015, 5 (3): 1–9.

[47] R. G. Pearson, *Chemical Hardness* (Wiley, Hoboken, 1997).

[48] R. G. Pearson, *Proc. Natl. Acad. Sci*., 1986, 83, 8440–8841.

[49] Roncali J., *J. Acc. Chem. Res*. 2009, 42, 11, 1719–1730.

[50] Brédas, J. L. Silbey, R. Boudreaux, D. S. S., Chance, R. R., *J. Am Chem. Soc*., 1983, 105, 6555–6559.

[51] F. C. Grozema, L. P. Candeias, M. Swart, P. V. Duijnen, J. Wildemen, G. Hadzianon, *J. Chem. Phys*., 2002, 117, 11366–11378.

[52] J. Huang, Y. Niu, W. Yang, Y. Mo, M. Yang, Y. Cao, *Macromolecules,* 2002, 35, 16, 6080–6082.

[53] A. Gadisa, M. Svensson, M. R. Anderson, O. Inganas, *J. Appl. Phys. Lett*., 2004, 84, 1609–1611.

[54] C. Deibel, T. Strobel, V. Dyakonov, *Adv. Mater*., 2010, 22 (37), 4097–4111.

[55] Qiang Mei; Mingwei Shan; Liying Liu; Guerrero, J. M., *IEEE Transactions on Industrial Electronics*, 2011, 58 (6), 2427–2434.

[56] Y. He, H. Y Chen, J. Hou, Y. Li, *J. Am. Chem. Soc*., 2010, 132, 1377–1382.

[57] Chemissian v. 4.01 demo version. Available online at: http://www.chemissian.com.

[58] D. Porath, G. Cuniberti, R. Di Felice, *Top. Curr. Chem*. 237 (2004) 183–228.

[59] H. J. Son, W. Wang, T. Xu, Y. Liang, Y. Wu, G. Li, L. Yu, *J. Am. Chem. Soc*. 2011, 133, 1885–1894.

[60] L. G. Mercier, A. Mishra, Y. Ishigaki, F. Henne, G. Schulz, P. Bäuerle, *Org. Lett*. 2014, 16, 2642–2645.

[61] G. J. Hedley, A. J. Ward, A. Alekseev, C. T. Howells, E. R. Martins, L. A. Serrano, G. Cooke, A. Ruseckas, I. D. W. Samuel., *Nat. Commun*. 2013, 4 (1), 2867.

[62] X. He, S. Mukherjee, S. Watkins, M. Chen, T. Qin, L. Thomsen, H. Ade, C. R. McNeill., *J. Phys. Chem. C*. 2014, 118, 9918–9929.